Quantum thermalization dynamics with Matrix-Product States

Eyal Leviatan,[1] Frank Pollmann,[2,3] Jens H. Bardarson,[2,4] and Ehud Altman[5]

[1]*Department of Condensed Matter Physics, Weizmann Institute of Science, Rehovot 7610001, Israel*
[2]*Max-Planck-Institut für Physik komplexer Systeme, Nöthnitzer Str. 38, 01187 Dresden, Germany*
[3]*Technische Universität München, Physics Department T42, 85747 Garching, Germany*
[4]*Department of Physics, KTH Royal Institute of Technology, Stockholm SE-10691, Sweden*
[5]*Department of Physics, University of California, Berkeley, CA 94720*

arXiv:1702.08894v1 [cond-mat.stat-mech] 28 Feb 2017

We study the dynamics of thermalization following a quantum quench using tensor-network methods. Contrary to the common belief that the rapid growth of entanglement and the resulting exponential growth of the bond dimension restricts simulations to short times, we demonstrate that the long time limit of local observables can be well captured using the time-dependent variational principle. This allows to extract transport coefficients such as the energy diffusion constant from simulations with rather small bond dimensions. We further study the characteristic of the chaotic wave that precedes the emergence of hydrodynamics. Both the "butterfly velocity" and the Lyapunov exponent are shown to converge with rather small bond dimension.

The question how quantum systems thermalize, or fail to do so, when evolving under their own intrinsic dynamics is an important challenge for theoretical physics, which recently came within the reach of experiments in ultra-cold atomic systems [1–6]. Recent studies of holographic models [7–9] as well as certain exactly solvable strongly coupled field theories, such as the Sachdev-Ye-Kitaev model [10–14], have uncovered a wealth of emergent structure in the dynamics of thermalizing systems that has not been appreciated before and is beyond the semiclassical Boltzmann description of thermalization. For example, these studies have suggested the existence of fundamental quantum bounds on transport, thermalization rates and chaotic dynamics. These new results also lead to conjecture possible universal relations between the characteristics of chaos which determine the rate of information scrambling in a system and hydrodynamic transport coefficients that control the long time relaxation of physical observables [15].

The new ideas on quantum thermalization need to be tested with generic physical models and this, in turn, requires new methods for computing quantum time evolution. Almost all the numerical calculations done so far to address this problem relied on exact diagonalization (see e.g.[16–20]), which is severely constrained by the attainable system sizes. On the other hand, the density matrix renormalization group (DMRG) [21] and other tensor network based methods can tackle large systems, but are considered inadequate for computing the long time dynamics. The main obstruction is the rapid growth of entanglement entropy, which translates to exponential growth with time of the tensor (bond) dimensions needed for the calculation [22].

In this paper, we propose a way to overcome the limitation on computation of long time dynamics within the manifold of tensor networks. A first clue that something is amiss in the usual assessment of the entanglement growth as a fundamental obstruction comes from the observation that quantum thermalizing systems are governed at long times by emergent classical hydrodynamics. Given the universality of the hydrodynamic behavior, dictated by conservation laws and a small number of parameters, we do not expect the dynamics of local observables to depend on the detailed long range entanglement structure of the micro-state. The pertinent question then is how to truncate the growing entanglement entropy without sacrificing crucial information on local observables?

Previous attempts to restrain the growth of entanglement entropy involved the use of matrix-product operators (MPO) [23] or purified states [24–27] to represent density matrices. These works sought to utilize an inherent advantage in using thermal density matrices rather than pure states: while in pure states the thermodynamic entropy is encoded entirely through long range quantum correlations (entanglement entropy), in a density matrix it can be represented as a statistical mixture of local degrees of freedom (or local entanglement with ancila bits in a purified state). Thus, for example, the infinite temperature density matrix is simply a unit matrix, equivalent to a direct product of unit matrices representing the local mixed states. When perturbed by a local operator at the origin (e.g. by imposing a spin up there), such a system is expected to relax back to effective local equilibrium over a short timescale set by the local interactions. One might hope that the local equilibrium state attained in the process can again be described in terms of an MPO (or purified state) with short range quantum correlations, similar to the initial state. Unfortunately, the exact time evolution leads to linear growth of the entanglement entropy of the density matrix in time. Attempts to curb the entanglement growth, while still capturing the exact density matrix, have met with only partial success, allowing to reduce the growth rate somewhat [23, 26, 27]. But the fundamental problem of an exponentially growing bond dimension remains.

Here we take a different approach, which aims to truncate the entanglement growth within a systematic ap-

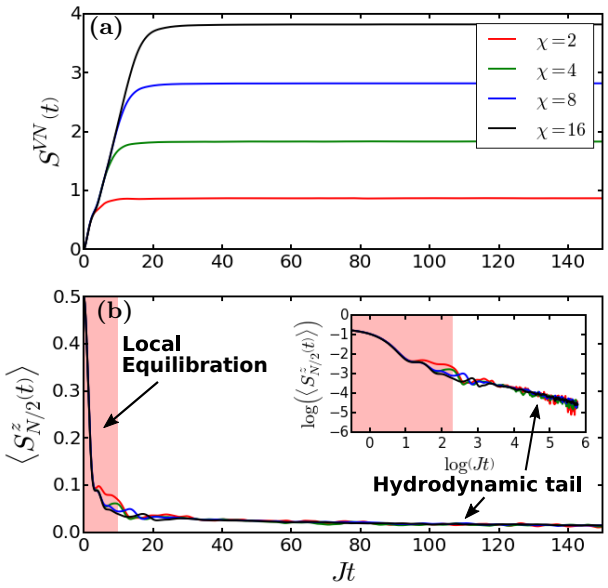

FIG. 1. (a) Half-system entanglement entropy following a quantum quench to an initial ensemble of random product states. As expected the entropy increases linearly in time and saturates to a value roughly equal to log of the bond dimension χ. (b) Relaxation dynamics of the perturbed middle spin in the same calculations. A fast decay which leads to local equilibration is seen at short times followed by a slow hydrodynamic (diffusive) tail decaying as $1/\sqrt{t}$. The inset shows the decay on a log-log scale emphasizing the long time tail.

proximation, rather than attempting to capture the exact dynamics. To this end we employ the time dependent variational principle (TDVP) [28, 29] to time-evolve matrix product states (MPS) [30] within a space of fixed bond dimension χ, using an efficient algorithm proposed by Haegemann *et. al.* [31, 32] (see also [33, 34]). The entanglement entropy in this approach is capped by $\log\chi$. Hence, the MPS is not even a nearly approximate description of the micro-state, which would naturally evolve to volume law entanglement entropy. In the language of time dependent MPS calculations, the truncation error is bound to become large after a short time.

Why then should the TDVP scheme nonetheless capture the long time dynamics of thermalizing systems? A crucial feature for our purpose is that the TDVP respects conservation laws regardless of the truncation. This is in contrast to the common time dependent DMRG methods (such as the time evolving block decimation (TEBD) [35]) which violate them when the truncation error becomes large. Indeed the TDVP generates non-linear classical dynamics in the variational manifold, driven by a classical Hamiltonian having the same symmetries as the original quantum Hamiltonian. Because such non linear dynamics is generically chaotic, the hydrodynamic behavior of local observables is guaranteed to emerge at long times even if we only keep a small bond dimension. Of course, we are not guaranteed a priori that the hydrodynamics in this scheme is governed by the correct transport coefficients. On physical grounds, however, we expect that these are determined by quantum processes that occur on rather short scales related to the short thermalization time and possibly the thermal coherence length. Such processes can in principle be captured by MPS with finite bond dimension. Increasing the bond dimension of the variational family of states allows to systematically improve the calculation and to assess the accuracy of the result by checking for convergence with χ.

To test the new approach, we consider the dynamics of the Ising chain with both longitudinal and transverse fields:

$$H = J\sum_{i=0}^{N-1} S_i^x S_{i+1}^x + h_x \sum_{i=0}^{N} S_i^x + h_z \sum_{i=0}^{N} S_i^z. \qquad (1)$$

Here S_i^α are spin-1/2 operators defined on site i. This model, in a regime of parameters far from any integrable point, is commonly used as a testbed for thermalization dynamics [36, 37]. A simplifying feature is the lack of symmetries, which leaves energy as the only conserved quantity. In our calculations $N = 100$ (i.e. the chain length is 101 sites) and we use the coupling constants: $\{J, h_x, h_z\} = \{4, 1, -2.1\}$, for which the system is indeed far from any integrable point and shows fast thermalization [36]

We use the TDVP to compute the dynamics induced by application of a local perturbation to a thermal ensemble of initial states, as explained in more detailed below. We compute two types of quantities. First we look at relaxation of local observables following the quench to find the expected long time tails associated with energy diffusion. From this we extract the energy diffusion coefficient. Second, we compute diagnostics of chaos from which we extract a Lyapunov exponent and a "butterfly velocity" associated with the ballistic propagation of the chaos front. Both types of quantities appear to converge well with bond dimension χ.

Method – We now describe the application of the TDVP approach to the problem in some more detail. As mentioned, the TDVP imposes classical dynamics in a phase space defined by the parameters of a variational state $|\,\psi[\alpha]\,\rangle$ through the effective Lagrangian:

$$\mathcal{L}[\alpha,\dot{\alpha}] = \langle\,\psi[\alpha]\,|\,i\partial_t\,|\,\psi[\alpha]\,\rangle - \langle\,\psi[\alpha]\,|\,H\,|\,\psi[\alpha]\,\rangle \qquad (2)$$

In our context the variational manifold is the space of MPS with fixed bond dimension χ:

$$|\,\psi\,\rangle = \sum_{\sigma_1\cdots\sigma_N} A^1_{\sigma_1}\cdots A^N_{\sigma_N}\,|\,\sigma_1\cdots\sigma_N\,\rangle \qquad (3)$$

The variational time evolution is implemented in each time step δt through application of effective *single site*

evolution operators on all the matrices $A^1_{\sigma_1}$ to $A^N_{\sigma_N}$ in succession, as described in Ref. [32]. The effective single site evolution operator is obtained from an effective single site Hamiltonian generated by contracting, from both sides, the underlying Hamiltonian with the truncated MPS having the matrix corresponding to that site removed.

Our goal is to compute the evolution of a local perturbation applied to a thermal ensemble. Thus, we compute time dependent quantities following a quench as averages over an ensemble of initial states. The initial states are chosen to represent the suitable canonical ensemble, perturbed by the application of a local operator on the middle of the chain.

As a first demonstration of the method we start from a sample of random product states with the direction of the spin on each site chosen independently from a uniform distribution on the Bloch sphere. At this point the ensemble represents the infinite temperature state. The ensemble is quenched by application of the single site operator $S^+_{N/2}$ on the middle site of the chain (followed by normalization), to every state in the ensemble. The states of the quenched ensemble are then evolved using the TDVP scheme with a given fixed bond dimension χ.

Fig. 1(a) shows the average entanglement entropy of the evolved states. The MPS entanglement entropy is seen to grow linearly in time and saturate to the maximum value possible for the given bond dimension $S \to \log_2 \chi$. Hence the curves corresponding to different values of χ depart strongly from each other. In contrast the relaxation of the local operator $S^z_{N/2}$ on the quenched site, seen in Fig. 1(b), has quantitatively the same behavior for the different values of χ.

We see two stages in the relaxation of $S^z_{N/2}$. First is a rapid decay of the expectation value as the system reaches local thermal equilibrium on a few microscopic time units. The second stage, seen more clearly in the inset of Fig. 1(b) is a power law decay of the residual spin expectation value. This is the expected hydrodynamic long time tail. Note that S^z is not conserved, the hydrodynamic tail arises because this operator has a finite overlap with the energy density; it is a manifestation of energy diffusion in the system. This is a first demonstration that such long time thermalization dynamics can be captured accurately using low entanglement states.

For a more accurate study of the thermalization dynamics in what follows we use a different ensemble of initial states. Instead of taking a sample of random product states we consider fully random MPS of fixed bond dimension χ right at the outset. That is, we do not restrict the initial states to be product states. This has the advantage that each state of this ensemble is in itself more representative of the infinite temperature state as it typically corresponds to the maximal entanglement entropy for the given χ. This facilitates faster convergence

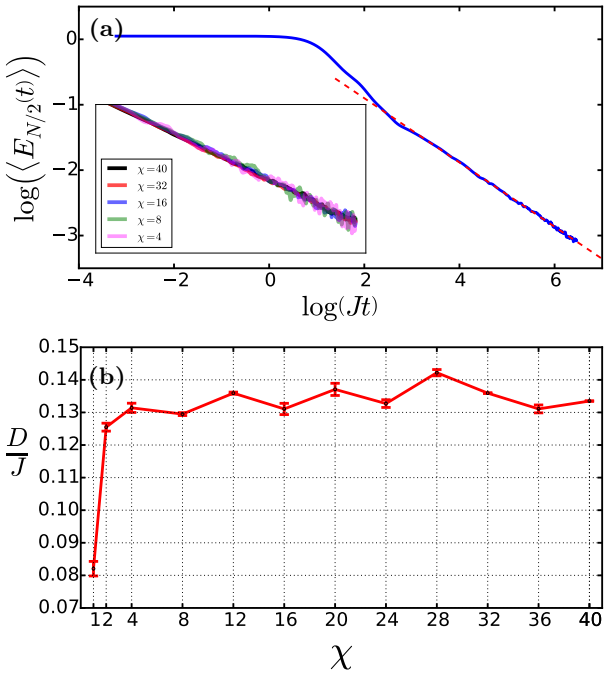

FIG. 2. (a) Decay of the energy on the middle site of the chain after the quench agrees perfectly with a diffusive decay as $\sim 1/\sqrt{t}$. This plot corresponds to bond dimension $\chi = 32$. Similar behavior is seen for different χ. (b) The diffusion constant extracted from the energy relaxation computed with different bond dimensions shows convergence beyond $\chi \approx 4$.

with sample size. As before, the quench operator S^+_n is applied to the middle site for every state (followed by normalization) to produce the ensemble of initial states.

Before proceeding we note that it is possible to similarly study a quench of a finite temperature state. This is done by evolving the random MPS in imaginary time (and normalizing the state) before applying the quench operator. In this paper, however, we we focus on thermalization and chaotic dynamics at infinite temperature.

Energy diffusion – The diffusive tail observed in the relaxation of a local observable emerges because that observable has a finite overlap with the local energy. The perturbation $S^+_{N/2}$ applied to the thermal state has injected energy to locally in the middle of the chain. Because of energy conservation, this excess energy is expected to spread out diffusively away from the perturbed site at long times with a profile:

$$E(x,t) = \frac{E_0}{\sqrt{2\pi D t}} \exp\left(-\frac{x^2}{2Dt}\right) \tag{4}$$

where x is the distance from the middle site. This is indeed the behavior found in the calculations, which show, for all bond-dimensions, a decay of the energy of the middle site ($x = 0$) as $1/\sqrt{t}$. Fig. 2(a) depicts an example of the energy relaxation on the middle site, obtained

from averaging over 1000 random initial MPS of bond-dimension $\chi = 32$. Note the separation of time scales between a fast decay to local equilibrium, which happens over a time of order J^{-1} and the slow hydrodynamic decay that sets in afterward. The diffusion constant extracted from the fit to Eq. (4) for $x = 0$ is seen in Fig. 2(b) for bond dimensions 1 through 40. The result shows rapid convergence with bond dimension for $\chi \geq 4$. Note that we gradually reduced the number of initial states averaged over as we increased the bond dimension. Specifically we used 6000 initial states for $\chi = 1, 2$ and gradually went down to 500 initial states for $\chi = 36, 40$, where the calculations are most demanding. We note, however, that at high bond dimension the state to state fluctuations are much smaller and thus they require less averaging.

The errors in fitting the diffusion constant are estimated by the following procedure. We add simulated Gaussian noise to the average curve of $E(x = 0, t)$ with an amplitude determined by the variance of shot to shot fluctuations in this quantity and a correlation time of $10/J$. We fit the diffusion constant from an ensemble of such simulated noisy curves in order to assess the fit error.

Quantum chaos – The emergence of hydrodynamic transport is closely linked to quantum chaos. Hydrodynamics can ensue only if the dynamics becomes effectively irreversible through the scrambling of information by chaos. Below we characterize the chaotic dynamics in our model.

As a first step we define a diagnostic of chaos which is convenient to compute with MPS. Classical chaos is characterized by exponential divergence of nearby phase space trajectories. Quantum wavefunctions cannot diverge from each other in the same way because the unitary evolution preserves distance in Hilbert space. Instead, let us consider states of a subsystem, described by the appropriate reduced density matrices. A measure of distance between these two reduced states can diverge when the system as a whole is undergoing quantum unitary evolution similarly to the divergence of classical trajectories.

For concreteness consider the spin model (1) with the quench scheme used for the above calculations. For each state in the ensemble of initial conditions we wish to compare the time-evolutions of the unperturbed state denoted by $|\psi_1\rangle$ with that of the perturbed state $|\psi_2\rangle = S^+_{N/2}|\psi_1\rangle$. For this purpose we consider the Schmidt decomposition of the two time-evolved states taken at a bi-partition of the chain at site $l = N/2 + x$.

$$|\,\psi_a(t)\,\rangle = \sum_j \lambda_{a,j}(x,t)\,|\,\psi^L_{a,j}(x,t)\,\rangle\,|\,\psi^R_{a,j}(x,t)\,\rangle \qquad (5)$$

Let us define the partial overlap matrix: $M_{ij}(x,t) \equiv \langle \psi^R_{1,i}(x,t)\,|\psi^R_{2,j}(x,t)\rangle$. Then a valid distance measure between the states reduced to the right bi-partition is

$$\begin{aligned} d^2(x,t) &\equiv \mathrm{tr}\left[(\rho^R_1(x,t) - \rho^R_2(x,t))^2\right] \\ &= \sum_{i,a} \lambda^4_{i,a} - 2\sum_{ij} \lambda^2_{i,1}\lambda^2_{j,2}|M_{ij}|^2 \end{aligned} \qquad (6)$$

However, for simplicity, we will consider a non-weighted version of the distance measure given by:

$$d^2_M(x,t) = 1 - \chi^{-1}\mathrm{tr}\left[M^\dagger M\right] = 1 - \chi^{-1}\left\|M\right\|^2 \qquad (7)$$

In our case these two distance measures are almost proportional to each other because from the start the random MPS correspond to states with almost maximal entanglement entropy, so that $\lambda^2_{i,a} \approx \chi^{-1}$ for all i and a.

We note that the distance measure (6) can be measured by interfering two copies of the time dependent quantum state [38], using the experimental set-up developed to measure the second Renyi entropies in Ref. [39]. For example, to measure the overlap $\mathrm{tr}(\rho^R_1\rho^R_2)$ one would needs to perturb only one of the two copies at $t = 0$, before interfering them at time t [40].

Fig. 3 (a) presents the dependence of $\chi^{-1}\left\|M\right\|^2$ on the distance and time from the quench event. The calculation was done with bond dimension $\chi = 16$ and averaged over 500 random initial states, however, similar results are obtained for different values of χ as we discuss below. The chaotic dynamics is expected to manifest in an exponential collapse of this overlap that propagates with a velocity v_B, known as the "butterfly velocity" after the butterfly effect, from the point of the perturbation. The ballistic propagation is indeed immediately apparent in the colormap image.

To better characterize the chaos we plot the growth of the distance measure Eq. (7) taken at different spatial distances x from the perturbation. As seen in Fig. 3(b), all lines collapse perfectly, after shifting the time axis by x/v_B, on a universal function growing as:

$$d^2_M(x,t) = f_0 \exp\left[\lambda_L\left(t - \frac{x}{v_B}\right)\right] \qquad (8)$$

from which we can extract the Lyapunov exponent λ_L. Fig. 4(a) shows the convergence of λ_L with bond-dimension.

The butterfly velocity extracted from the ballistic propagation of the chaotic wave, $v_B = 0.454$ (in units of Ja), is found to be larger than the velocity implicit in the linear growth of the entanglement entropy $v_E \equiv dS_{VN}/dt \approx 0.238$ shown in Fig. 1 (a). This is in agreement with the predictions of Ref. [41], which argued that the entanglement velocity, being constrained by strong sub-additivity, must be smaller than the speed of operator spreading [42]. For a certain idealized model, Ref. [41] even found a factor of two between the two velocities, similar to our result. Note that the butterfly velocity that we measure is expected to approach the

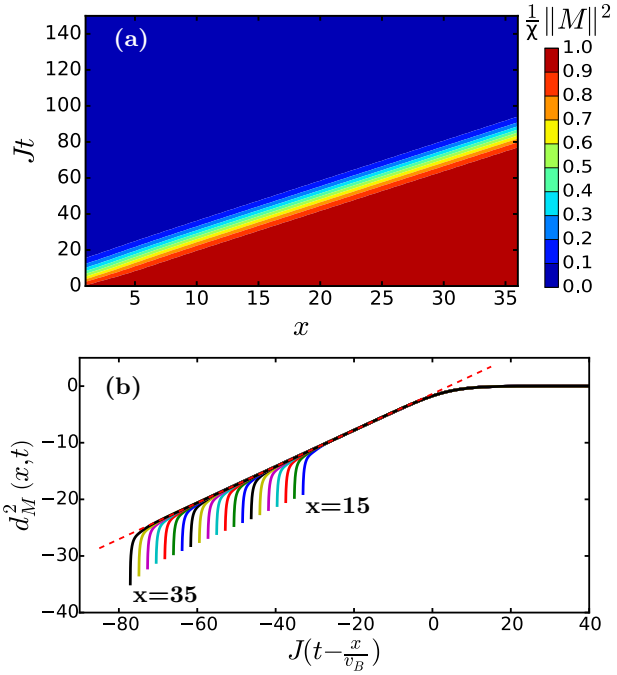

FIG. 3. (a) A colormap of the partial overlap used as a diagnostic for quantum chaos (see text) clearly shows ballistic propagation with of the chaotic wave with a velocity v_B known as the "butterfly velocity". This is in contrast to the diffusive energy transport in the system. (b) Plots of $d_M^2(x,t)$, a measure of the distance between the perturbed and unperturbed reduced state at different distances x from the perturbation as a function of the shifted time coordinate $t - x/v_B$. The different plots are collapsed on each other with a single fitting parameter v_B and follow an exponential divergence with a Lyapunov exponent λ_L.

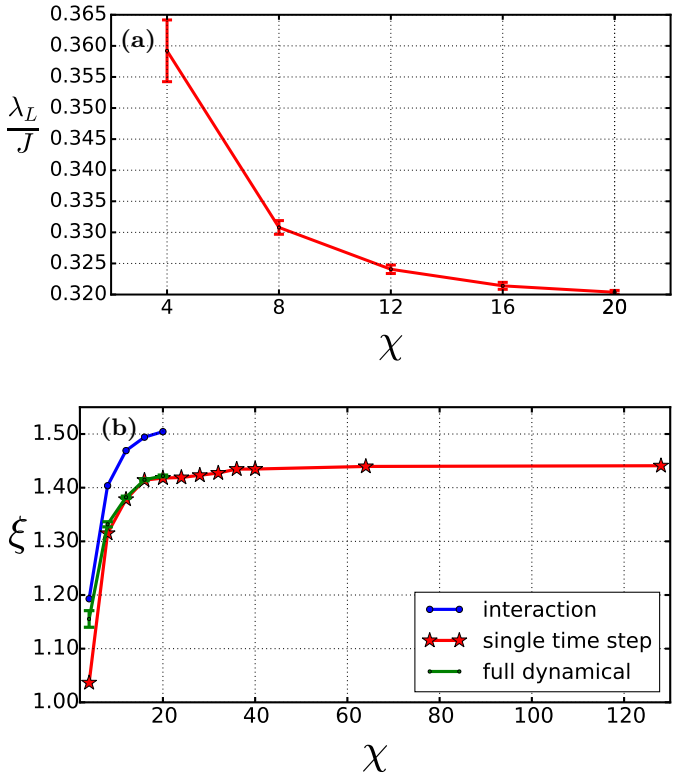

FIG. 4. (a) Convergence of the calculated value of λ_L with bond dimension. (b) The length scale $\xi = v_B/\lambda_L$ found by computing v_B and λ_L independently from the full dynamics (green) is compared to the scale ξ found directly from the spatial dependence decay of d_M after a single time step (red). The latter can be related to the length scale associated with the exponential decay of the interactions in the effective classical hamiltonian (blue). The three length scales appear to converge similarly with bond dimension.

speed of operator spreading in the high temperature limit in which we work here [37].

Another perspective on the propagation of chaos is gained by viewing the spatial dependence of $d_M^2(x,t)$ in the calculation, i.e. $\exp(-x\lambda_L/v_B)$, as a pre-existing difference between the two reduced states, which seeds the exponential divergence between them. If so, we should be able to obtain just the length scale $\xi = v_B/\lambda_L$ by looking at $d_M^2(x,\delta t_0)$ after a single time step. The result is plotted in plotted in Fig. 4(b) and compared to the ratio v_B/λ obtained from the full dynamics.

This instantaneous non-local influence of the perturbation, exponentially suppressed with distance, is related to the non-local interactions between the variational parameters in the classical Hamiltonian $\mathcal{H} = \langle\psi|H|\psi\rangle/\langle\psi|\psi\rangle$ that generates the dynamics according to Eq. (2). Those interactions can be estimated from the the second order variation of the energy

$$V_{ij} = \left\| \frac{\partial^2 \mathcal{H}\left[A^1,\ldots,A^N\right]}{\partial A^i \partial A^j} \right\| \sim e^{-|i-j|/\xi} \qquad (9)$$

where $A^1,\ldots,A^N$ are the matrices appearing in the MPS $|\psi\rangle$ and $\|\cdot\|$ denotes the Frobenius norm of the tensor. We find an excellent match between the scale ξ obtained in this way and that obtained from computing the dynamics.

The scale ξ which sets the range on which entanglement can significantly influence the dynamics of local observables can in principle depend on both the state and the Hamiltonian. For the random MPS we use here we see that ξ converges and becomes essentially independent of the state beyond a modest bond dimension; it therefore depends only on the Hamiltonian, which dictates a scale of order 1. The scale ξ is expected to increase, however, if we use MPS representative of lower temperature states (e.g. random MPS evolved by $e^{-\beta H}$). In particular we conjecture that ξ roughly follows the thermal correlation length as the temperature is lowered below the scale $\|H_{ij}\| \approx J$. This may suggest an exponential increase of the needed bond dimension χ_* with decreasing temperature.

Discussion – We have shown that calculations using the time dependent variational principle (TDVP) with rather low bond dimension matrix-product states (MPS), can capture the essential long time dynamics of thermalizing (closed) quantum systems at high temperature. This runs contrary to the conventional wisdom that the rapid growth of entanglement entropy severely limits the utility of tensor network calculations at long times. Indeed hydrodynamic behavior is naturally obtained in our calculations, allowing to extract transport coefficients such as the energy diffusion constant. We also obtain the characteristics of the chaotic wave that propagates ballistically and precedes the emergence of hydrodynamics. Both the "butterfly" velocity and the Lyapunov exponent characterizing the quantum chaos show rapid convergence with the bond dimension used in the calculation.

A crucial feature of TDVP in this context is that it satisfies energy conservation and other conservation rules. For this reason emergence of hydrodynamic behavior is essentially guaranteed for any bond dimension. The correct transport coefficients and chaos parameters are obtained in spite of the truncation because at high temperature they are generated by quantum processes on a short scale that can be captured by MPS with low bond dimension. The accurate results obtained at very low bond dimension (even $\chi = 2$) lends hope that this method may also be useful for computing the dynamics of systems in two or three dimensions.

It would be interesting to apply this method also to study the dynamics at finite temperature, especially in the vicinity of quantum critical points, where the system remains strongly coupled down to the lowest temperature. Calculations in this regime may allow to test conjectured quantum limits on transport as well as relations between transport and quantum chaos. We note however, that a larger bond dimension would be needed to capture quantum entanglement over the growing thermal coherence length, making these calculations more demanding.

The convergence of the chaos parameters with increasing bond dimension raises interesting questions concerning the crossover from classical to quantum chaos. For low bond dimension the TDVP constitutes non-linear classical dynamics of almost local variables. The emergence of chaos is then governed by the non linearity. On the other hand at the highest possible bond dimension the TDVP gives the exact many-body quantum dynamics, which is linear. This can still be viewed as classical Hamiltonian dynamics but in an enormous space of highly non-local variables. In this limit the chaotic dynamics is a result of coarse graining this huge space. It is reasonable to expect that the thermal coherence length provides a natural coarse graining scale on which it is possible to describe quantum chaos using non-linear classical equations.

Another interesting application of the method is to study the many-body localization transition at infinite temperature by approaching it from the thermal regime. In this case the calculation will become more demanding because of the need to capture the entanglement in the rare insulating inclusions (Griffith regions). The size of such regions grow together with the diverging correlation length $l_G \sim \xi \log(L/a)$, where ξ is the correlation length, on approaching the MBL critical point [43, 44].

Acknowledgements – This work has benefited from stimulating discussions with Erez Berg, Mark Fischer, Andrew Green, Markus Greiner, Anatoli Polkovnikov, and Mike Zaletel. We thank Ashley Milsted for discussions on the implementation of TDVP and for sharing his code. This research was supported in part by the ERC synergy grant UQUAM, Research Unit FOR 1807 through grants no. PO 1370/2-1 and by the ERC starting grant QUANT MATT no. 679722, and the National Science Foundation under Grant No. NSF PHY-1125915.

[1] L. Sadler, J. Higbie, S. Leslie, M. Vengalattore, and D. Stamper-Kurn, Nature **443**, 312 (2006).
[2] T. Kinoshita, T. Wenger, and D. S. Weiss, Nature **440**, 900 (2006).
[3] N. Strohmaier, D. Greif, R. Jördens, L. Tarruell, H. Moritz, T. Esslinger, R. Sensarma, D. Pekker, E. Altman, and E. Demler, Phys. Rev. Lett. **104**, 080401 (2010).
[4] M. Gring, M. Kuhnert, T. Langen, T. Kitagawa, B. Rauer, M. Schreitl, I. Mazets, D. A. Smith, E. Demler, and J. Schmiedmayer, Science **337**, 1318 (2012).
[5] M. Schreiber, S. S. Hodgman, P. Bordia, H. P. Lüschen, M. H. Fischer, R. Vosk, E. Altman, U. Schneider, and I. Bloch, Science **349**, 842 (2015).
[6] H. P. Lüschen, P. Bordia, S. Scherg, F. Alet, E. Altman, U. Schneider, and I. Bloch, arXiv preprint arXiv:1612.07173 (2016).
[7] P. K. Kovtun, D. T. Son, and A. O. Starinets, Phys. Rev. Lett. **94**, 111601 (2005).
[8] S. A. Hartnoll, Nature Physics **11**, 54 (2015).
[9] J. Maldacena, S. H. Shenker, and D. Stanford, Journal of High Energy Physics **2016**, 1 (2016).
[10] S. Sachdev and J. Ye, Phys. Rev. Lett. **70**, 3339 (1993).
[11] A. Kitaev, Talks at KITP, April 7, 2015 and May 27, 2015 .
[12] J. Maldacena and D. Stanford, (2016), arXiv:1604.07818.
[13] Y. Gu, X.-L. Qi, and D. Stanford, ArXiv e-prints (2016), arXiv:1609.07832 [hep-th].
[14] R. A. Davison, W. Fu, A. Georges, Y. Gu, K. Jensen, and S. Sachdev, arXiv preprint arXiv:1612.00849 (2016).
[15] M. Blake, Phys. Rev. Lett. **117**, 091601 (2016).
[16] V. Oganesyan and D. A. Huse, Physical Review B **75**, 155111 (2007).
[17] M. Rigol, V. Dunjko, and M. Olshanii, Nature **452**, 854 (2008).
[18] Y. Bar Lev, G. Cohen, and D. R. Reichman, Phys. Rev. Lett. **114**, 100601 (2015).
[19] K. Agarwal, S. Gopalakrishnan, M. Knap, M. Müller, and E. Demler, Physical review letters **114**, 160401 (2015).

[20] W. Fu and S. Sachdev, arXiv preprint arXiv:1603.05246 (2016).
[21] S. R. White, Phys. Rev. Lett. **69**, 2863 (1992).
[22] T. c. v. Prosen and M. Žnidarič, Phys. Rev. E **75**, 015202 (2007).
[23] M. C. Bañuls, M. B. Hastings, F. Verstraete, and J. I. Cirac, Physical review letters **102**, 240603 (2009).
[24] A. E. Feiguin and S. R. White, Phys. Rev. B **72**, 220401 (2005).
[25] T. Barthel, U. Schollwöck, and S. R. White, Phys. Rev. B **79**, 245101 (2009).
[26] C. Karrasch, J. Bardarson, and J. Moore, Physical review letters **108**, 227206 (2012).
[27] C. Karrasch, J. Bardarson, and J. Moore, New Journal of Physics **15**, 083031 (2013).
[28] P. A. Dirac, in *Mathematical Proceedings of the Cambridge Philosophical Society*, Vol. 26 (Cambridge Univ Press, 1930) pp. 376–385.
[29] R. Jackiw and A. Kerman, Physics Letters A **71**, 158 (1979).
[30] M. Fannes, B. Nachtergaele, and R. W. Werner, Commun. Math. Phys. **144**, 443 (1992).
[31] J. Haegeman, J. I. Cirac, T. J. Osborne, I. Pižorn, H. Verschelde, and F. Verstraete, Phys. Rev. Lett. **107**, 070601 (2011).
[32] J. Haegeman, C. Lubich, I. Oseledets, B. Vandereycken, and F. Verstraete, Phys. Rev. B **94**, 165116 (2016).
[33] K. Ueda, C. Jin, N. Shibata, Y. Hieida, and T. Nishino, eprint arXiv:cond-mat/0612480 (2006), cond-mat/0612480.
[34] J. M. Kinder, C. C. Ralph, and G. Kin-Lic Chan, ArXiv e-prints (2011), arXiv:1103.2155 [cond-mat.str-el].
[35] G. Vidal, Phys. Rev. Lett. **91**, 147902 (2003).
[36] M. C. Bañuls, J. I. Cirac, and M. B. Hastings, Phys. Rev. Lett. **106**, 050405 (2011).
[37] D. A. Roberts, D. Stanford, and L. Susskind, Journal of High Energy Physics **3**, 51 (2015), arXiv:1409.8180 [hep-th].
[38] A. J. Daley, H. Pichler, J. Schachenmayer, and P. Zoller, Phys. Rev. Lett. **109**, 020505 (2012).
[39] R. Islam, R. Ma, P. M. Preiss, M. Eric Tai, A. Lukin, M. Rispoli, and M. Greiner, Nature **528**, 77 (2015).
[40] We thank Markus Greiner for pointing out this possibility.
[41] A. Nahum, J. Ruhman, S. Vijay, and J. Haah, ArXiv e-prints (2016), arXiv:1608.06950 [cond-mat.stat-mech].
[42] We thank David Huse for alerting us to this point.
[43] R. Vosk, D. A. Huse, and E. Altman, Phys. Rev. X **5**, 031032 (2015).
[44] A. C. Potter, R. Vasseur, and S. A. Parameswaran, Phys. Rev. X **5**, 031033 (2015).